Volumetric and surface characterization of fly ash used as solidification agent for radioactive waste

[1]J. Bautista-Ruiz, [*2] W.A. Bautista-Ruiz, [3] M. Diaz-Lagos [4]S. A. Martinez-Ovalle

[1]*Departamento de Electricidad y Electrónica Facultad de Ingeniería, Universidad Francisco de Paula Santander, San José de Cúcuta, Norte de Santander, Colombia*

[*2]*Grupo de Física Nuclear Aplicada y Simulación, Escuela de Física, Universidad Pedagógica y Tecnológica de Colombia, Tunja, Boyacá, Colombia.*

[3] *Grupo de Ingeniería Geológica, Escuela de ingeniería geológica, Universidad Pedagógica y Tecnológica de Colombia, Sogamoso, Boyacá, Colombia.*

[4]*Grupo de Física Nuclear Aplicada y Simulación, Escuela de Física, Universidad Pedagógica y Tecnológica de Colombia, Tunja, Boyacá, Colombia.*

Abstract- **In this work, a combination of complementary volume and surface techniques was explored to evaluate the physicochemical properties of fly ash samples from a thermoelectric plant in Boyacá, Colombia. Used as fixed agent the radioactive isotopes The samples were classified as class F ash, with crystalline phases of mullite, quartz and hematite phases identified By X-ray diffraction (XRD). The distributions of particles present in fly ash are characterized by having a range of hydrodynamic diameters between 0.305 μm and 0.785 μm measurements made using Dynamic Light Scattering (DLS). Hollow spherical symmetry particles with a porous structure were observed, as well as wide particle size spherical particles by polished thin section (PTS) and scanning electron microscopy (SEM). Through z potential measurements, it was shown that the ash with pH>9 had the highest zeta potential value (-50 mV) and consequently the highest repulsive forces between particles and the greatest stability of the suspension. The BET active surface area of these samples was 6 m2/g. The properties of the samples, including crystallography, spherical morphology, small particle size, electrical characteristics of the surface and their application in the production of cement, can be used as a compound that helps.**

Keywords – X-ray methods, Al_2O_3, Nuclear applications, fly ash.

I.   Introduction

In an industrial context, fly ash (FA) is very fine waste, friable in nature, gray in color and soft to the touch. This type of material results from the combustion of pulverized coal in thermoelectric plants. Its composition and both physical and chemical properties depend on the type of coal, its origin, as well as the technological processes used in these plants. Taking as a reference to a plant in Colombia, for every 1500 tons of coal 200 tons of ash are produced per day. [1-3]

Although FA is a waste material, end-use markets for coal combustion products have developed and investigated applications in various fields due to both its physical and chemical characteristics [4-7]. Some application sectors are the cement industry, [8-14]; the construction and metallurgical industry [15-17] and environmental remediation [18-22]. Within this last field, the applications offered by FAs are varied, highlighting the fixing or adsorption of industrial waste such as mercury, phosphates, organic components of water, motor oils, and the immobilization and stabilization of radioactive waste [19, 24-27].

Immobilization is understood as the process in which waste, in this case, liquid and radioactive, is incorporated or converted into a solid, stable and chemically inert matrix. Immobilization is a set of physical and chemical methods that allow solidification or stabilization of residues. Stabilization is a general term by which techniques or methods are described by which waste is converted into a more stable form. This is normally achieved by adding reagents

that improve their handling and physical characteristics, reducing the release surface of the contaminants present in the waste.

In the development of this investigation, characterization techniques were used to determine the chemical composition, mineralogy, and surface properties of Colombian FA from the Boyacá region. The results allow establishing the potential use of the FA as a solidify agent of liquid radioactive waste.

II. Materials and methods

The samples of fly ash (FA) were supplied by the Compañía Eléctrica de Sochagota SA, Termopaipa IV located in Boyacá, Colombia.

2.1 Characterization in the volume of the FA

For the determination of the composition and concentration of the oxides present in the FA samples, a PANalytical energy dispersed X-ray fluorescence spectrometer, Axios Petro model of 4 kV was used with a Xenon (Xe) detector of flow scintillation and Rhodium (Rh) anode. Additionally, and parallel to the XRF analysis, a loss on ignition (LOI) analysis was performed at 105 °C following the ASTMD 7348 standard [28].

The mineralogical analysis of the FAs was developed using a PANalytical diffractometer, Empyream model in θ-2θ mode. The measurement was taken with Kα1 radiation (λ = 1.7890 Å) using the Bragg-Brentano geometric configuration, with a scanning speed of 0.013°/160 s and tube voltage of 45 kV, in a range between 2θ = 10° and 2θ = 70°. The Rietveld analysis was performed with the freely available Gsas software.

The size (hydrodynamic diameter) and the size distribution of the FA particles were determined using the DLS technique. The suspension of the particles was achieved using a solution of water and KCl as a dispersing medium in a concentration of 10^{-3} Molar. The measurement was made at a temperature of 25 °C and a detector count rate of 242.200 counts/second. The measurement time was 70 s. The equipment used was Malvern Zeta Sizer Nano ZS, which combines laser doppler velocimetry and scattered light phase analysis (PALS).

2.2 Surface characterization of FA

To obtain information on the morphology of the FAs and estimate the composition of the sample, the petrographic analysis was performed by light microscopy, using the polished thin section (PTS) technique with transmitted light. The components present were analyzed using a Leica DM 4500P polarized light petrographic microscope following ASTM D2797 [29].

The morphological characterization and chemical composition were developed in a Field Emission Scanning Electron Microscopy (FE-SEM) model Nova Nano SEM 230. The voltage applied in the range 50 V to 30 kV.

The semi-quantitative determination of the composition and electronic structure of the sample was performed using X-ray Photoelectron Spectroscopy (XPS) in an ultra-high vacuum (UHV) chamber with a base pressure of 10-10 mbar. The angle between the hemispherical analyzer (SPECS-PHOIBOS100) and the plane of the surface was maintained at 60° and the X-ray radiation was the Kα line of magnesium (Mg) (1253.6 eV). The bond energy scale (BE) was calibrated for carbon (C) 1s for 285 eV. The reference spectrum was recorded with an energy step size of 40 eV; and an energy step size of 0.25 eV for high-resolution spectra. The binding energy scale (BE) was calibrated for carbon (C) 1s for 285 eV. The analysis of the XPS results was carried out with the Casa XPS software. XPS data were performed with magnesium anode (Mg) Kα; the background signal from the spectrum was subtracted using a Shirley routine.

The Z potential measurement was performed with the Malvern Zeta Sizer Nano ZS equipment, this equipment employs a combination of laser doppler velocimetry and scattered light phase analysis (PALS), the suspension of the particles, was achieved using a solution of water and KCl as dispersing medium concentration of 10^{-3} Molar.

Nitrogen adsorption-desorption isotherms were captured at 77 K on a MICROMERITICS 3FLEXTM surface characterization kit, in a relative pressure range (P/Po) from 0.0025 to 0.95. The samples were weighed in 9 mm diameter cells made of MICROMERITICS borosilicate glass. Then the degassing was carried out with temperature (120 °C) and vacuum pressure (6 Pa) of the samples, this was carried out in the Vac Prep 061 MICROMERITICS

unit. Data analysis was performed in MICROMERITICS 3FLEX V.3.02 software. Before this, the sample underwent a pretreatment process that consisted of degassing at 120 °C and a pressure of 6 Pa for 12 hours.

The determination of the specific area was made by the BET method (Brunauer-Emmett-Teller) whose application interval was adjusted according to the consistency criterion of the Rouquerol transform. The pore size distribution was made by the BJH method (Barrett-Joyner-Halenda). The BET and BJH methods are included in MICROMERITICS software 3FLEX V.4.03, following the ISO 9277: 2010 standard [32].

III. RESULTS AND DISCUSSION

3.1. Chemical and mineralogical composition

Table 1 shows the main compounds (expressed as oxides) and the composition expressed as a percentage by weight (% Wt), compared with works that have proposed FA for applications for the immobilization of radioactive waste; It is noteworthy that the sum of the elemental oxides in this work is not equal 100% due to the presence of trace elements not commonly reported in this type of ash [29].

Table 1 Compositional analysis of fly ash in decreasing order of concentration

Compound Chemical	SiO_2	Al_2O_3	Fe_2O_3	K_2O	CaO	TiO_2	P_2O_5	Na_2O	MgO	SO_3	SrO	BaO	CuO	V_2O_5	Zr_2O_2	LOI
(% Wt)	64.90	25.00	5.01	1.40	1.30	1.20	0.70	0.50	0.41	0.13	0.11	0.10	0.09	0.05	0.03	8.11

It is observed that these FAs contain other elements in a lower quantity and a considerable high value of losses by ignition close to 12%.

According to the ASTM C618 Standard, it is possible to classify these ashes as type F by the sum of $SiO_2 + Al_2O_3 + Fe_2O_3$ oxides > 70%, the classification of type F ash was confirmed by XRF.

The presence of calcium oxide (CaO) in the FA gives them a basic character, this as long as the presence of this is superior to that of the oxides of aluminum (Al_2O_3), silicon (SiO_2), and iron (Fe_2O_3) which give an acid character to this material. As can be seen in Table 1, said oxides are superior to calcium, therefore the ash analyzed is acidic in nature [32,33]

When comparing the percentages by weight obtained in this investigation with those reported by [19-24], which are works in applications for the immobilization of radioactive waste, it is observed that the vast majority of oxides have percentages slightly higher than analyzed in this work. [24] Has stated that FA used in place of cement is an optimal material for the immobilization of radioactive waste. Considering the results, it is possible to affirm that the studied FA are useful for the manufacture of cement due to the presence of aluminosilicates that react better with calcium hydroxides (Ca (OH)$_2$) [33].

In general, coal combustion residues contain more than 80% of vitreous silico-aluminous material, which makes it possible for them to be used as raw materials for high-value adsorbents, immobilizers and construction materials [34].

Figure 1 shows the XRD spectra (a) within the already refined pattern (b) of the FA sample, the symbols: (M), (Q), (H) represent the phases of Mullite Quartz and Hematite, respectively.
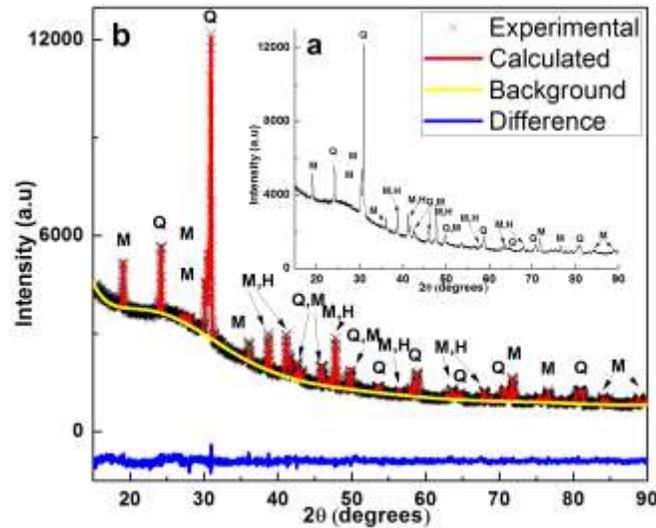
Figure 1.   XRD spectra recorded of the FA (a) diffractogram FA (b) diffractogram adjusted by Rietveld refinement

Figure 1 shows that the samples analyzed are mainly composed of silicon, aluminum, and iron oxides, which give rise to crystalline phases related to Mullite ($Al_{4.80}O_{9.60}$ $Si_{1.20}$) with 58% crystallized in an ortho-rhombic phase with space group Pbam (# 55). A Quartz (SiO_2) phase with 37% crystallized in a trigonal phase P3121 (# 152) and finally, a Hematite (Fe_2O_3) phase with 5% crystallized in a trigonal phase with space group R-3CH (# 167). These results agree with other investigations that establish the majority presence of mullite and the low content of calcium oxide that this type of FA possesses [1,2, 11, 35-37].

Crystalline phases such as Mullite and Quartz would allow chemical interaction so that radioactive waste components are immobilized in crystalline quartz and mullite networks, making them part of the crystalline network when mixed and by temperature action they are linked, allowing to increase the stability of said residue [24].

3.2. The FA in aqueous medium: Dynamic Light Scattering

Figure 2 presents three measures of DLS for the same sample of FA. This study allowed us to observe that the FA present varied average hydrodynamic diameters. The results allow establishing the possible behavior of the FA when used as a stabilizer for liquid radioactive waste.
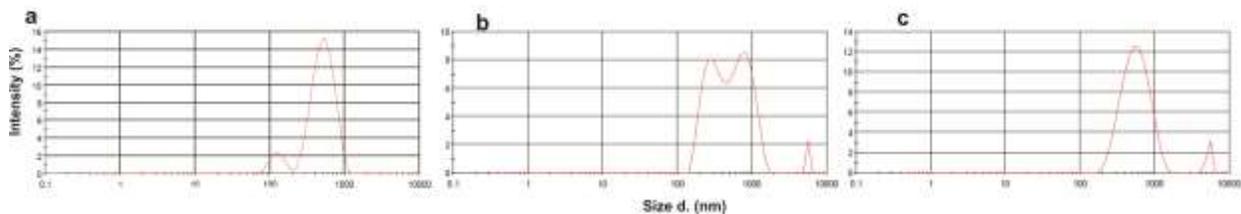

Figure 2.   Average diameter distributions of FA as a function of light percentage

Figure 2a shows a bimodal distribution with peaks at 126 nm and 532 nm, and percentages of intensities of 2% and 15%, respectively. Figure 2b shows a trimodal distribution with peaks at 305 nm, 785nm µm, and 5560 nm; with intensity percentages of 8%, 9%, and 2.1% respectively. Finally, figure 2c shows a bimodal distribution with representative peaks at 589 nm and 5301 nm. The intensity percentages are 13% and 3% respectively. Large differences in particle diameter distributions are also evident. This trend can be associated with the formation of aggregates of the particles with the liquid medium, forming aggregates with other particles and increasing their diameter. Some may remain non-interacting and therefore result in such large diameter size distributions, especially at peaks 3 of measure b and 2 of measure c.

Figure 2 shows the presence of peaks with low intensities as shown in the peak of measure 2a. This behavior can be explained as a low probability of agglomeration.

In general, the results allow us to infer that the most probable hydrodynamic diameter distributions of the FA when interacting with an aqueous medium are between 305 nm and 785 nm. These distributions can influence adsorption processes. It is known that the finer the FA particles, the greater their surface area and therefore the greater their reactivity. This reactivity occurs at the particle-liquid interface and would allow applications related to the stabilization of liquid radioactive waste.

3.3. Composition and morphology

The morphology of the FAs was characterized by PTS petrographic technique transmitted light. Additionally, the SEM technique was used to evaluate the samples in detail and to develop their chemical-qualitative analysis. Figure 3 shows a cenosphere with an average interior radius of 45 µm. The qualitative chemical analysis of the same sample is evidenced in Figures 4, 5 and 6, respectively.
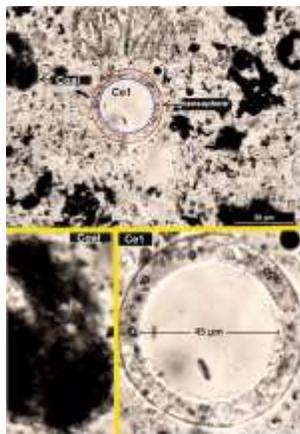

Figure 3.   Polished thin section optical image seen with transmitted light.
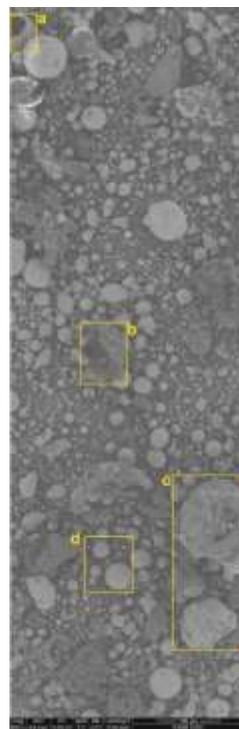

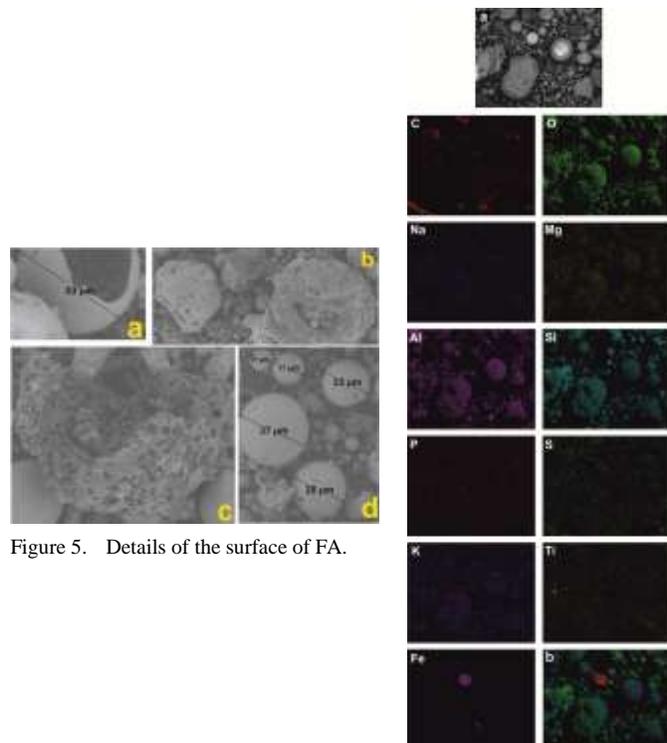Figure 4.   General morphology of a sample of FA.

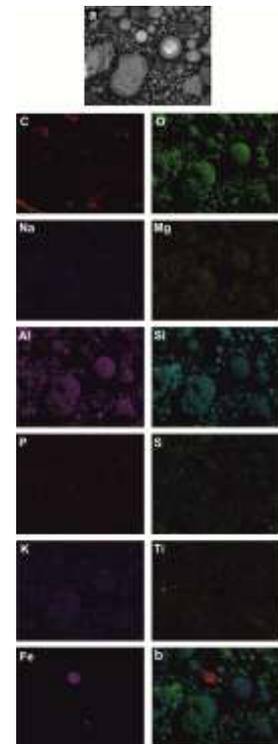Figure 5.   Details of the surface of FA.

Figure 6.   Chemical mapping of the surface of FA.

Morphological analysis revealed particles with spherical symmetry and broken with an average diameter of 53 µm. Hollow spheres, known as the plerosphere, are also observed with smaller spherical particles inside (Figure 5a). Irregular and porous particles are evident due to the presence of unburned coal. Also, agglomerates consisting of particles of various sizes closely linked by unburned coal are distinguished (Figure 5b and 5c), and spherical particles of wide particle size distribution with diameters of 11 µm, 17 µm, 23 µm, 28 µm, and 37 µm, Figure 5d, which can often be hollow or solid and are known as cenospheres.

Figure 6 shows the result of the identification of the chemical elements present in the FAs. This qualitative analysis was performed in the region observed in the micrograph of Figure 6 (a). The analysis revealed a high presence of elements such as oxygen (O), silicon (Si), aluminum (Al); to lesser extent magnesium (Mg), sulfur (S), potassium (K),

titanium (Ti), carbon (C) and iron (Fe), and presence, although very little sodium (Na) and phosphorus (P). Figure 6b shows the superimposition of images for the aforementioned elements.

In general, the analysis shows that the FAs are mainly made up of spherical symmetry particles, some hollow in the center and others irregular with a high content of oxygen, aluminum, and silicon.

The XPS analysis confirms that the main constituent elements of the near-surface region are: oxygen (43.0%), carbon (37.4%), silicon (11.9%), aluminum (5.1%), sulfur (1.4%), with small amounts of phosphorus (0.4), calcium (0.3%), nitrogen (0.3) and iron (0.2%). Similar results for FA samples have been reported by [38,39]. It is noteworthy from this analysis that elements such as silicon and aluminum are more significant than oxygen and carbon. The high concentration of silicon and aluminum can lead to the formation of aluminate and silicate groups, responsible for the negative charge on the surface [19].

Figure 7 shows the Zeta potential curve as a function of the pH of the suspension of FA particles in an HCL solution. It can be seen that in the FA the particles are positively charged at low pH values, negatively at high pH and zero charges (PZC) at a pH of 2.6. Therefore, charged metal ions are likely to adsorb to charged FA particles at a pH above 2.6. At a pH of approximately 9, the zeta potential registers the maximum value of -50mV due to greater repulsion forces between particles and greater stability of the suspension. The isoelectric point of the suspension was determined at a pH of 2.1. When hydrating the FA, its pH reached values between 9 and 10. This condition leads to a high degree of metal ion precipitation.

The FA surfaces are negatively charged of figure 7. This result is corroborated with other investigations [19]. However, in the present study, it was found that the analyzed FAs have a greater tendency to negatively charge at lower pH values. It is important to highlight that the main constituent compounds of FAs such as SiO_2 and Al_2O_3 determine the surface charge. Electrostatic interactions in aluminosilicates have a greater advantage with other types of radioactive waste stabilizers [40].
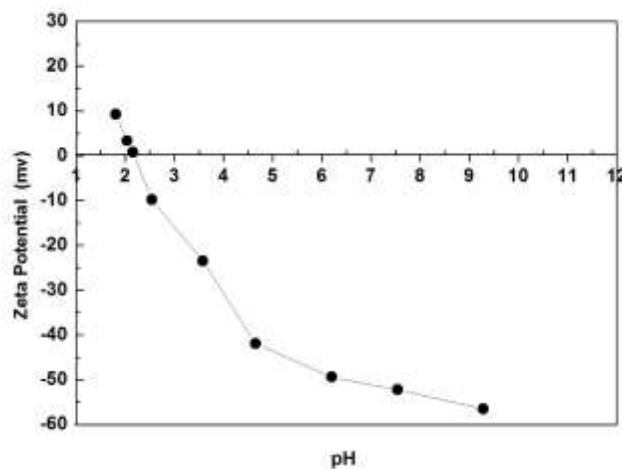

Figure 7.   Z potential values as a function of pH by adding KCL in FA samples.

For the analysis of the results of figure 7, the information on the variation of the surface charge of the FAs analyzed as a function of the pH value in an aqueous medium can be used. All substances have some pH value, including liquid radioactive waste, although it is not possible to control their pH value, in FAs it is possible to control these values, especially for these ashes whose nature is acid, obtaining a surface electric charge. that allows attracting radioactive waste.

The variation of the Z potential under the different pH conditions of the dispersant solution simulates the experimental conditions present in the ash-liquid radioactive waste interaction during the electrokinetic treatment. This result shows the usefulness of measuring the z-potential at different pH by predicting the solution conditions to be used in the development of the FA-radioactive liquid residue electrokinetics experiment.

3.3. Textural properties of fly ash: specific surface

Figure 8 shows the nitrogen adsorption (blue curve) and desorption (orange curve) isotherms for the FAs studied. The results establish a BET specific surface area of 6 m^2/g, a value consistent with that reported in other investigations for ash from the same region [41]. The nitrogen adsorption-desorption isotherm for fly ash can be classified as type II isotherm according to the IUPAC classification and is characteristic for non-porous materials with relatively small specific surface area, according to [42] the upward slope of almost all of the isotherm is due to adsorption in a multilayer monolayer on the stable, external surface of the solid without the presence of micropores or mesopores. This behavior is validated in the same figure 8 with that reported by [43], The abrupt growth behavior of the isotherm at relatively very low pressures indicates zero porosity of the sample.
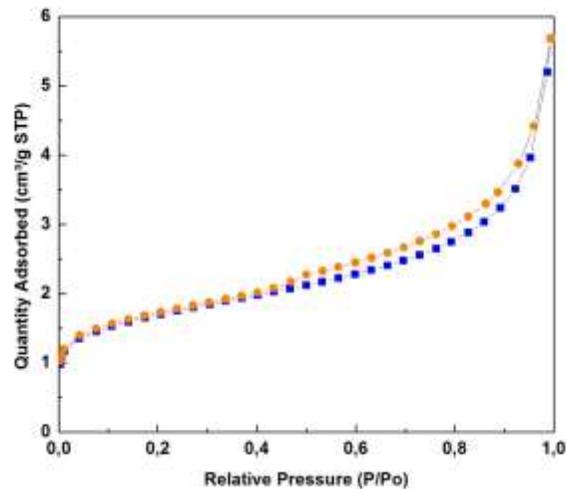

Figure 8. N_2 adsorption isotherm at 77K for the FA sample.

Through the adsorption isotherm and the low hysteresis that it presents, it is an indication of the no porosity or very little porosity of the FA. This behavior translates into that if they are used without making some kind of benefit to improve this characteristic, it is not possible to immobilize waste satisfactorily, due to the lack of places where liquid radioactive waste would be deposited; according to Santaella [2]; FA absorb water due to various characteristics, including its irregular and porous texture. The FA studied, being so little porous, reduces the absorption of water, which would result in little absorption of liquid radioactive waste.

The results show that the FAs are composed of aluminosilicates. This condition allows evaluating its great potential for use as a material for the immobilization of liquid radioactive waste because it promotes the origin of spherical symmetry particles, such as cenospheres and plerospheres. This type of particle composed of amorphous aluminosilicates facilitates the formation of aluminate and silicate groups responsible for the negative surface charge, allowing the surface of the FAs to interact with radioactive residues, particularly alpha particles, and immobilizing them.

Cenospheres and plerospheres are the main components for manufacturing containers where it is possible to dump radioactive waste in the liquid phase to subsequently sinter them and finally obtain immobilized waste.

IV. CONCLUSION

The analysis of XRF and XRD showed that the studied FAs are composed of class F aluminosilicates and, therefore, the formation of particles with a large composition of aluminum and silicon is promoted. In many cases, their symmetry is spherical, which allows them to be used as capsule for liquid radioactive waste and then they are sintered and obtain an immobilized residue.

Crystalline phases such as Mullite and Quartz found as techniques such as XRD could function as crystalline networks in which radioactive elements present in the liquid waste can be introduced into them, by sintering.

According to the results obtained by the BHJ method, the FA is a material that does not present porosity or very little porosity. which, if used solely for this characteristic, would not optimally immobilize liquid waste without first performing some kind of benefit, since being very little porosity there is a reduced number of spaces (pores) where radioactive liquid waste can be housed, to carry out immobilization of radioactive material.

The PTS micrographs together with the scanning electron microscopy images revealed the presence of different particle sizes, especially cenospheres and plerospheres that can serve as cavities to incorporate and then immobilize liquid radioactive waste.

The chemical analysis of the surface by XPS suggests that the main constituents of the surface besides oxygen and carbon, the presence of silicon and aluminum is evident. These elements promote the formation of aluminate and silicate groups that give rise to a negative electric charge, which was verified by analyzing the Z potential.

ACKNOWLEDGEMENT

REFERENCES

[1] Vassilev, V. S; Vassileva, G.C. (2007). A new approach for the classification of coal fly ashes based on their origin, composition. Fuel (86), 1490-1512.

[2] Santaella, E; (2001). Caracterización física química y mineralógica de las cenizas volantes. Cienc. Ing. Neogranadina, 10, 47-62.

[3] Reyes, F; Martinez, S. A; Moreno, M. (2015). Mossbauer characterization of feed coal, ash and fly ash from a Thermal power plant. Hyperfine Interact. 232, 141-148.

[4] Aperador, W; Ruíz, E; Delgado, A. (2014). Electrochemical Impedance Spectroscopy Analysis on Steel Embedded in a Concrete Alkali Exposed on the Chloride Media Int. J. Electrochem. Sci., 9, 7506 – 7517.

[5] Blissett, S. R; Rowson, A. N. (2012). A review of the multi-component utilization of coal fly ash. Fuel, 97, 1-23.

[6] Heidrich, C; Feuerborn J. H; Weir, A. (2013). Coal Combustion products: a global perspective. 2013 world of coal ash (WOCAA) CONFERENCE 1-17.

[7] Manz, O. E. (1999). Coal fly ash: a retrospective and future look. Fuel 78(2), 133–136.

[8] Akbar, A. (2014). Cement Replacement Materials, Springer-Verlag: Reading Berlin, 41-157

[9] Barrera, J.C. (2010) Análisis del comportamiento mecánico del cemento hidráulico adicionado con cenizas volantes provenientes de la central de generación térmica termopaipa, thesis Universidad Industrial de Santander, 15-20.

[10] Cifuentes, P.A; Ferrer, C.I. (2006). Análisis del comportamiento mecánico a edades tardías del concreto hidráulico con adición de cenizas volantes de termopaipa, Thesis   Universidad Industrial de Santander, 10-12.

[11] Pedraza, S; Pineda, P; Gutiérrez, O. (2015). Influence of the unburned residues in fly ash additives on the mechanical properties of cement mortars. Procedia Mater. Sci. 9496 – 503.

[12] Santaella, E. (2004), Comportamiento del concreto con bajos porcentajes de ceniza volante (Termopaipa IV) y agua constante. Cienc. Ing. Neogranadina, 14, 14-19.

[13] Shuang, Z. W. (2011). Influence of fly ash on the mechanical properties of frame concrete. Sustainable Cities and Soc. 1(3) 164–169.

[14] Valderrama, C. P; Torres, J; Mejía de Gutiérrez, R. (2011). Características de desempeño de un concreto adicionado con cenizas volantes de alto nivel de inquemado. Ing. e investigación, 31(1) 39-46.

[15] Castells, X.E. (2000). Reciclaje de Residuos Industriales, vol. 495, Díaz Santos, Madrid, 857-859

[16] Wang, S; Wu, H. (2006). Environmental-benign utilisation of fly ash as low-cost adsorbents. J. Hazard. Mater. 136(3) 482–501

[17] Rohatgi, P. K; Gupta, N; Schultz, F. B; Luong, D. D. (2011). The Synthesis, compressive Properties, and applications of metalmatrix Syntactic foams. The Journal of The Minerals, Met. & Mater. Society (TMS), 63(2) 36-42.

[18] Yao, Z.T; Ji X.S., Sarker, P.K; Tang, J.H; Ge, L.Q; Xia, M.S; Xi, Y.Q. (2015). A comprehensive review on the applications of coal fly ash. Earth Sci. Rev., 141. 105-121

[19] Lieberman, R. N; Green, U; Segev, G; Polat, M; Mastai,. Y H. Cohen. (2015). Coal fly ash as a potential fixation reagent for radioactive wastes. Fuel, 153(1) 437-444.

[20] Inada, M; Eguchi, Y; Enomoto, N; Hojo, J. (2005). Synthesis of zeolite from coal fly ashes with different silica-alumina composition. Fuel. 842 99-304.

[21] Oviedo Henao J.A; Reyes, C.A. (2012). A comparative study study on conversion of industrial coal by-products in low SiO2 Zeolite of faujasite type. Dyna, 176(79) 105-114.

[22] González, C. P; Montaño, A. M; Castro, D. C. (2012). Obtención y caracterización de geopolimeros, sintetizados a partir de ceniza volante y piedra pómez, utilizados para el desarrollo y mejoramiento del concreto. El hombre y la máquina, 38 59-65.

[23] Vassilev, S. V; Vassileva, C. G. (2005) Methods for Characterization of Composition of Fly Ashes from Coal-Fired Power Stations: A Critical Overview. Energy Fuels, 9(3) 1084–1098.

[24] Osmanlioglu, A.E; (2014). Utilization of coal fly ash in solidification of liquid radioactive waste from research reactor. Waste Manag Res. 32(5) 366-70

[25] Gilliam, T.M. (1991). Use of coal fly ash in radioactive waste disposal (EPRI-GS--7162-Vol2, United States, 37.1-37.8

[26] Vasilieva, N. G; Anshits, N. N; Sharonova, O. M; Burdin, V; Anshits, A. G; (2005). Immobilization of Cesium and Strontium Radionuclides in Framework Aluminosilicates with the Use of Porous Glass-Ceramic Matrices Based on Coal Fly Ash Cenospheres. Glass Phy. and Chem., 31(5) 637-647.

[27] Sheng, J; (2001). Vitrification of borate waste from nuclear power plant using coal fly ash. (I) Glass formulation development. Fuel, 80 1365-1369

[28] American Society for Testing and Materials (ASTM), (2013). D7348, Standard specification for coal fly ash and raw or calcined natural pozzolan for use in concrete Standard Test Methods for Loss on Ignition (LOI) of Solid Combustion Residues, 1-7.

[29] American Society for Testing and Materials (ASTM), (2004). D2797, Standard Practice for Preparing Coal Samples for Microscopical Analysis by Reflected Light, 1-10

[30] The International Organization for Standardization (ISO), 927 (2010), Determination of the specific surface area of solids by gas adsorption — BET method, 1-24

[31] Chancey, R. T; Stutzman P; Juenger, M.C.G; Fowler, D. W; (2010).Comprehensive phase characterization of crystalline and amorphous phases of a Class F fly ash, Cem. Concr. Res. 40 146–156.

[32] Goma, F. El cemento portland y otros aglomerantes, Editores técnicos asociados S.A: Reading, Barcelona, 1979.

[33] Bautista Ruiz, W. A; Díaz, M; Martínez, S.A. (2017). Caracterización de las cenizas volantes de una planta termoeléctrica para su posible uso como aditivo en la fabricación de cemento. Rev. investig. desarro. innov, 8(1) 135-146.

[34] Wojciech, F; Wiatros, M.M; Magdalena, W. (2015). Coal fly ash as a resource for rare earth elements. Environ Sci Pollut Res, 22 9464–9474.

[35] Xue, Q; Lu, S. (2008). Microstructure of ferrospheres in fly ashes: SEM, EDX and ESEM analysis. Journal of Zhejiang University Science A, 9(11) 1595-1600.

[36] Rashad, A. M; Ouda, A.S. (2016). An investigation on alkali-activated fly ash pastes modified with quartz powder subjected to elevated temperatures. Constr. Build. Mater. 122 417-425.

[37] Franus, W. (2012). Characterization of X-type zeolite prepared from coal fly ash. Pol. J. Environ Stud. 21(2) 337–343.

[38] Van der Merwe, E.M; L. Prinloo, C; Mathebula, C.L; Swart,H.C; Coetsee, E; Doucet, F.J. Surface and Bulk characterization of an ultrafine south African coal fly ash wuth reference to polymer applications. Appl. Surf. Sci. 317(2014) 73-83.

[39] Chujiang, C; Shen, Z; Wang, M; Shuling, Ma; Xing, (2003). Surface metallization of cenospheres and precipitators by electroless plating. China particuology, 1(4) 156-161.

[40] Jang, J.G; Park, S. M; Lee, H. K; (2017). Cesium and Strontium Retentions Governed by Aluminosilicate Gel in Alkali-Activated Cements. Mater. 10(4) 1-13.

[41] Umaña, J. C., (2002) Síntesis de zeolitas a partir de cenizas volantes de termoeléctricas del carbón, Ph.D. Thesis, Universitat Politécnica de Catalunya Barcelona Tech., 212-215

[42] De Santiago, C. (2015) La fisisorción de nitrógeno. Fundamentos físicos, normativa, descripción del equipo y procedimiento experimental, Centro de Estudios y Experimentación de Obras Públicas (CEDEX): Reading Madrid, 18-21.

[43] Kulatos, I. Y.M., Gao, R.H Hurt, EM. Suuberg, (2001).Adsorption of ammonia on coal fly ash. Proc. 2001 International Ash Utilization Symposium, 59, 1-10